THE JOURNAL OF THE ACOUSTICAL SOCIETY OF KOREA VOL.24, NO.1E 2005, 3 pp. 21~27

Matched Field Processing: Ocean Experimental Data Analysis Using Feature Extraction Method

Kyungseop Kim*, Woojae Seong*, Heechun Song**
*Dept. of Naval Architecture and Ocean Engineering, Seoul National University, Seoul, KOREA
**Marine Physical Lab., UCSD, La Jolla, CA USA
(Received September 30 2004; accepted December 20 2004)

Abstract

Environmental mismatch has been one of important issues discussed in matched field processing for underwater source detection problem. To overcome this mismatch many algorithms professing robustness have been suggested. Feature extraction method (FEM) [Seong and Byun, IEEE Journal of Oceanic Engineering, 27(3), 642-652 (2002)] is one of robust matched field processing algorithms, which is based on the eigenvector estimation. Excluding eigenvectors of replica covariance matrix corresponding to large eigenvalues and forming an incoherent subspace of the replica field, the processor is formulated similarly to MUSIC algorithm. In this paper, by using the ocean experimental data, processing results of FEM and MVDR with white noise constraint (WNC) are presented for two levels of multi-tone source. Analysis of eigen-space of CSDM and FEM performance are also presented.

Keywords: *Matched field processing, Environmental mismatch, Feature extraction method (FEM), MVDR with white noise constraint*

I. Introduction

Matched field processing (MFP)[1,2] utilizes pressure field replicas to match the measured signals. Because of this inherent trait, mismatch problem has been one of important issues of MFP for underwater source detection. A propagation model for the replicas requires having accurate a priori knowledge of the physical properties of the ocean. However, it is costly to obtain accurate environmental information because of stochastic nature of real ocean environment. In order to overcome this mismatch, many researches for robust algorithm, e.g., multiple constraint method (MCM)[3] and minimum variance- environmentally perturbed constraint (MV-EPC)[4], have been performed. Also, probabilistic techniques, e.g., optimum uncertain field processor (OUFP)[5] and feature extraction method (FEM)[6], have been proposed with the aim of improving robustness on environmental mismatch.

In this paper, we present MFP results with real ocean experimental data using FEM and MVDR with white noise constraint (WNC)[7,8]. FEM is one of the robust MFP algorithms, which is based on the eigenvector estimation. Using the uncertain environmental parameters which are randomly sampled, the multiple replica signal vectors can be obtained for each candidate source position. With these replica vectors, a covariance matrix is constructed and decomposed to extract the eigenvectors. The eigenvectors corresponding to large eigenvalues can be deemed as the signal components for each assumed replica position. By excluding these eigenvectors and forming an incoherent subspace of the replica field, the processor can be formulated similarly to MUSIC algorithm. Although this method requires multiple acoustic propagation solution modeling over varying environmental parameter space, it is robust to the environmental mismatches and maintains good

Corresponding author: Woojae Seong (wseong@snu.ac.kr)
Dept. of Ocean Engineering, Seoul National University, Shillim-dong Kwanak-ku, Seoul, 151-742, Korea

sidelobe suppression capability[6]. WNC is one of most widely used processors because it provides some flexibility in setting the trade-off between robustness of conventional (Bartlett) processor and sidelobe suppression capability of MVDR processor. The results of WNC are presented here to be compared with FEM performance.

The rest of this paper is organized as follows, in Section II, we will briefly review the two processors - FEM and WNC. In Section III, a description of the experimental data is presented. The experiment was performed in a shallow water coastal environment with vertical line array. The source has two levels of multi-tone frequencies and the processing was performed for each levels. For each frequency tones, the ambiguity surfaces are compared. In second level tones, incoherent summation of FEM and WNC results are demonstrated. Analysis for eigen-space of CSDM and FEM performance are also presented. The results and discussion are presented in Section IV. Finally, in Section V, we presented a summary and conclusions on our findings.

II. Processing Algorithms

2.1. WNC Adaptive Processor

Adaptive processor has higher sidelobe suppression capability than conventional processor. But adaptive processor is also sensitive to mismatches thus source detection may not be possible with inaccurate environmental information. WNC processor is based on minimum variance distortionless response (MVDR) processor. Adding the white noise constraint to optimization process for MVDR processor, the weight vector of WNC processor is given by

$$\mathrm{w} = \frac{(\mathbf{R}+\varepsilon\mathbf{I})^{-1}\mathrm{d}}{\mathrm{d}^{H}(\mathbf{R}+\varepsilon\mathbf{I})^{-1}\mathrm{d}} \tag{1}$$

where R is CSDM and is usually estimated by averaging snapshots. I is the identity matrix and d is the steering vector or replica vector. The weight vector has the operational diagonal loading factor of ϵ to control the white noise gain. The weight vector w satisfies the white noise constraint for each steering direction such that

$$\delta^2 < \mathrm{G}_w = \frac{1}{|\mathrm{w}^H \mathrm{w}|} < \mathrm{N} \tag{2}$$

where N is the number of sensors. In practice, white noise gain (WNG) value is used in normalized form as

$$\mathrm{WNG} = 10\log\left(\frac{\delta^2}{N}\right) \le 0\,\mathrm{dB} \tag{3}$$

where WNG = 0 dB corresponds to a conventional processor and WNG = $-\infty$ dB corresponds to a pure MVDR processor. In this paper WNG = -2 dB will be used in the data processing, which is an appropriate level for balancing between robustness and sidelobe suppression capability.

2.2. Feature Extraction Method

FEM is based on eigenvector estimation. By extracting a common feature from the multiple replica signals for each assumed source position, the robustness for environmental mismatches can be achieved. Let H be a $N\times M$ matrix whose columns are the replica vectors for an assumed source position, A, with different environmental parameter values

$$\mathbf{H}(A) = [\mathrm{H}_1\,\mathrm{H}_2\cdots\mathrm{H}_M] \tag{4}$$

where N is the number of phones and M is the number of random perturbation of the environmental parameters. With this matrix, we can construct the covariance matrix of replica field, E(A), which contains information about the pressure field generated by source located at a replica position A, and subsequently obtain the eigenvector expansion of the matrix

$$\mathbf{E}(A) = \mathbf{H}\mathbf{H}^H = \sum_{i=1}^{N} \lambda_i \mathrm{V}_i \mathrm{V}_i^H \tag{5}$$

And then, the eigenvectors with relatively large eigenvalues can be said to be the main features of the pressure field generated by a source located at the assumed replica position, i.e., they represent the possible signal vectors at the replica position. Using the remaining eigenvectors corresponding to smaller eigenvalues, we can

construct a subspace that is almost orthogonal with the true replica vector. We can also define the $N \times N$ constraint matrix whose column space is the same as the subspace spanned by smallest eigenvectors. We obtain a matrix which contain the $(N-k)$ eigenvectors corresponding to the smallest eigenvalues as follows

$$\mathbf{E}_s(A) = [\mathrm{V}_{k+1}\, \mathrm{V}_{k+2} \cdots \mathrm{V}_{N-1}\, \mathrm{V}_N] \tag{6}$$

where E_S is obtained by removing the eigenvectors corresponding to k largest eigenvalues in E. The number of removed eigenvalues is determined based on the problem at hand by trial and error[6]. Usually it is selected to be the same or below the number of dominant modes propagating in the waveguide. Using this reduced matrix E_S, we can construct the constraint, E_L, as

$$\mathbf{E}_L(A) = \mathbf{E}_s \mathbf{E}_s^{H}. \tag{7}$$

And then FEM processor is given by

$$B(A) = \frac{1}{\mathbf{P}^{H}\, \mathbf{E}_L\, \mathbf{P}} \tag{8}$$

where P is the received field data. Because it was falsely charged to construct received signal vector P and average it over snapshots from time series of raw data, we used eigenvector decomposition of snapshot-averaged CSDM in order to construct the signal vector P. Snapshot-averaged CSDM, R, can be decomposed as follows;

$$\mathbf{R} = \sum_{snapshot} \mathrm{P}\mathrm{P}^{H} = \sum_{i=1}^{N} \phi_i \Phi_i \Phi_i^{H} \tag{9}$$

and then received signal vector which is averaged over snapshots is represented as

$$\mathrm{P} = \sum_{i=1}^{N_s} \sqrt{\phi_i}\, \Phi_i \,. \tag{10}$$

III. Experimental Data

The data used in this paper are from the SWellEx-96 experiment. The experiment was conducted in May 1996, 12 km off the coast of San Diego in California. A vertical line array was deployed from the FLIP (FLoating Instrument Platform) spanning a depth ranging from 94 m to 212 m. A total of 64 sensors were arranged at regular intervals, but only 21 sensor outputs were used in the processing. The bathymetry of the area where the experiment was conducted, and ship tracks are shown in Figure 1. Figure 2 shows the typical downward refracting summer sound speed profile of this area.

A Source was tracked at 5 knots along the iso-bath and the nominal depth of the source was 60 m. And an

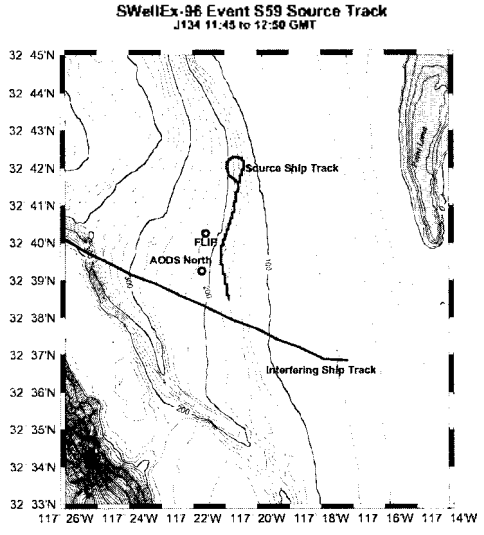

Fig. 1. Topography of the SWellEx-96 experiment site and ship tracks.

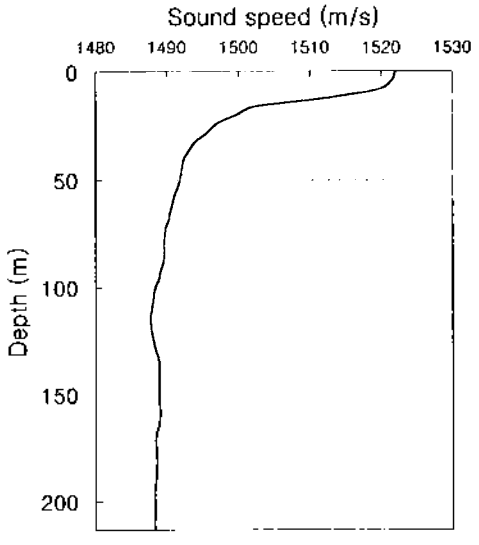

Fig. 2. Sound speed profile of the SWellEx-96 experiment site.

Table 1. Frequency tones of source and interference.

		Frequency (Hz)
Source (60 m)	High level	49 64 79 94 112 130 148 166 201 235 283 338 388
	2nd level	52 67 82 97 115 133 151 169 204 238 286 341 391
Interference		53 54 56 59 60 62 66 69 72 74

interfering ship was passing along the track on the South side of the FLIP. The source had a total of five-levels of multi-tones, but the data was processed for the first and second level tones. Each signal level was composed of 13 tonal frequencies. High level signal spanned from 49 Hz to 388 Hz and the second level signal had 3 Hz additive frequency bins to that of high level signal. The interference also showed multi-tones at low frequency band. Frequency information of source and interference is represented in Table 1.

IV. Source Localization Results

We used normal mode propagation model, ORCA[9] to construct replicas. Because of iso-bath source track, we used a range independent model. The time duration of processed signal was 60 sec. and sampling rate was 1500 Hz (i.e. a length of total data sequence is 90000). The FFT length was 9000 with Hanning window and there was 50 % overlap between successive snapshots.

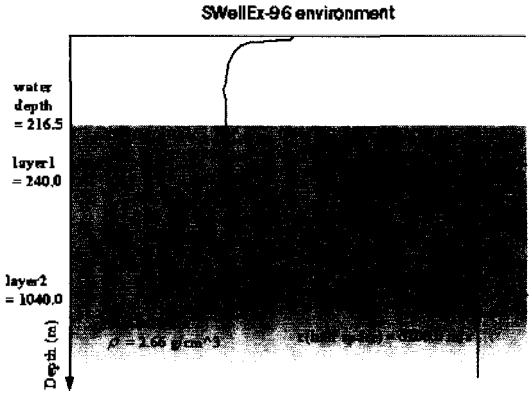

Fig. 3. Environmental bottom parameters for the SWellEx-96 experiment, based on direct measurements and bottom inversion.

4.1. High Level Signal

First, let us assume that the accurate (or best-available) environmental parameters are known. Figure 3 shows the three layer bottom model and geoacoustic parameters from previous measurement and inversion. Figure 4 shows each ambiguity surfaces of Bartlett, WNC, and FEM for high level signal tones of frequencies 49, 130, and 235 Hz. The results of Bartlett processor are presented here for comparison. Due to high SNR, all the results of three processors have peaks at the true source position. The range-depth ambiguity surfaces of Bartlett have the mostsidelobes. On the other hand, those of WNC and FEM

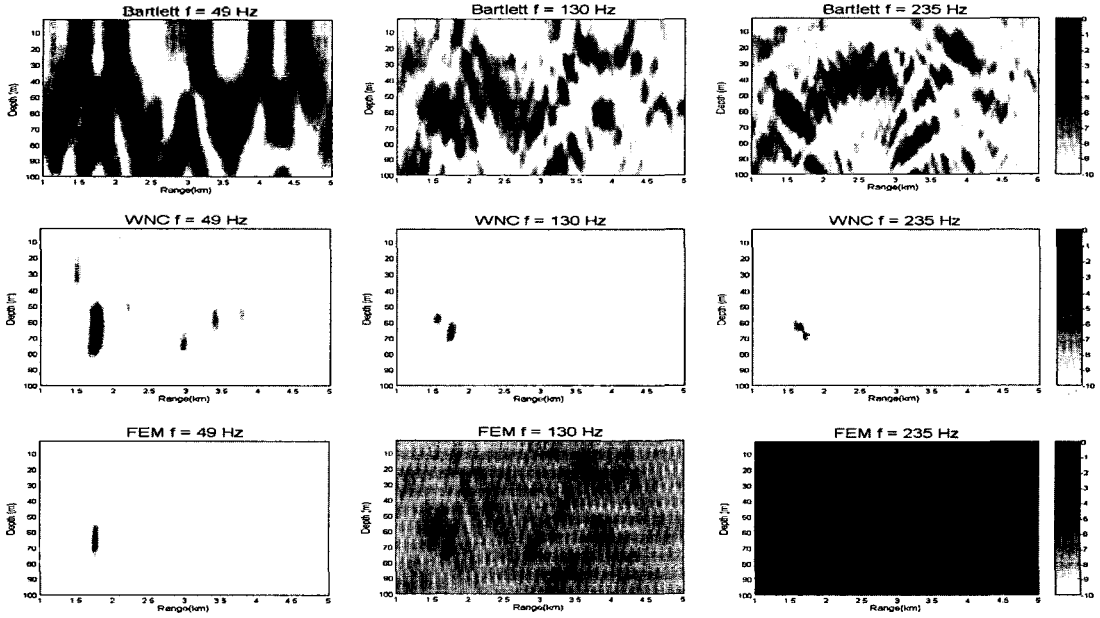

Fig. 4. MFP ambiguity surfaces for high level signal (tones of 49, 130, 235 Hz) when environmental parameters have no mismatch. FEM used the fixed one replica set (M=1, k=1). Dynamic range is 10 dB.

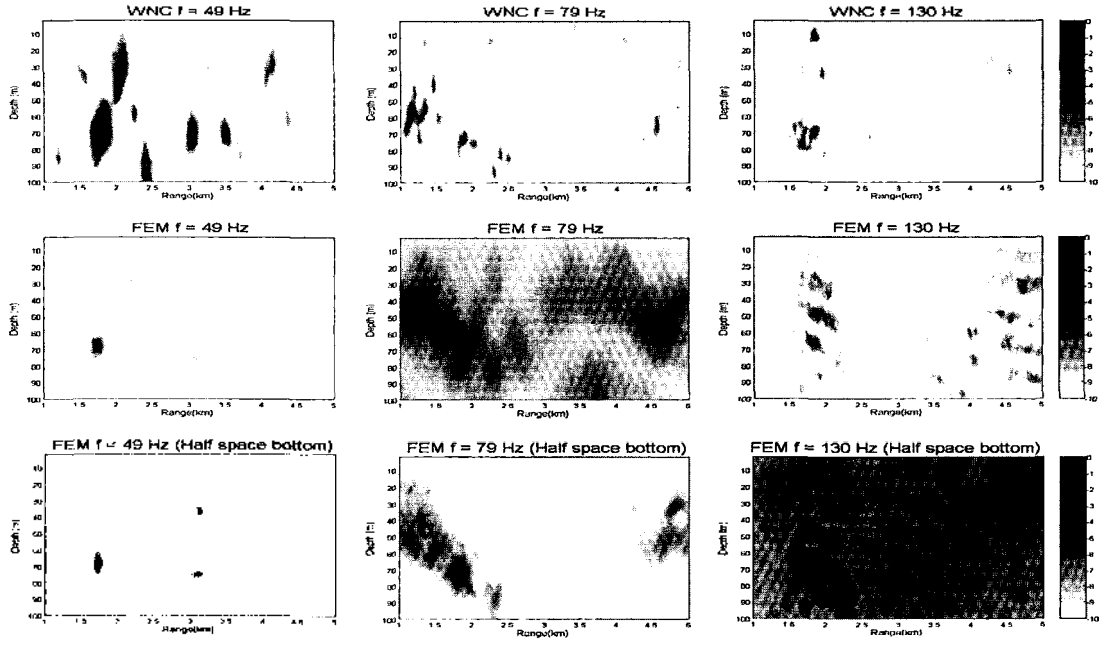

Fig. 5. MFP ambiguity surfaces for high level signal (tones of 49, 79, 130 Hz) when mismatch is severe (at first and second rows of figures). FEM used - 49 Hz: M=20, k=2/ 79 Hz: M=30, k=2/ 130 Hz: M=30, k=10. The figures of third row are results of half space bottom case (49 Hz: M=20, k=2/ 79 Hz: M=30, k=2/ 130 Hz: M=30, k=2). Dynamic range is 10 dB.

show localization results with relatively good sidelobe suppression. But, in FEM results, the peak to noise field ratio is lower as frequency becomes higher. In case where accurate (or deterministic) environmental information is known, FEM uses one fixed replica set and eliminate one largest eigenvector (M=1 and k=1). Because there are relatively many components of propagating mode at high frequency, the elimination of one largest eigenvector is not sufficient to make whole null space. So this produces low peak to noise field ratio in FEM ambiguity surfaces. The ambiguity surfaces for other frequency bins of 13 tones showed similar results (but are not shown here).

Figure 5 shows the results of the case where environmental mismatch is severe. When mismatch is slight, WNC also showed robust results as good as FEM. However, with severe mismatch, WNC does not show good localization performance. The results of low frequency tones were especially affected by mismatch in first bottom layer parameters of layer height, density, attenuation and compressional wave speed. Yet FEM results still show good localization performance. For this mismatch scenario, we constructed replicas using perturbed environmental parameters. The magnitudes of perturbation are shown in Figure 6. For processing with WNC, only one set of parameters which were randomly selected within this range was used for replicas. And M random set of parameters were used to constitute the replica set of FEM. The number of eigenvectors to eliminate (k in Eq. 6) was selected to be the same or below the number of dominant modes propagating in the waveguide[10]. Since at higher source frequency more number of propagating modes are present in the waveguide, the available number of eigenvectors to eliminate increase as frequency rises.

Note the ambiguity surfaces of the third row in Figure 5. They are FEM processing results using half space bottom model for construction of replicas. We can see that they

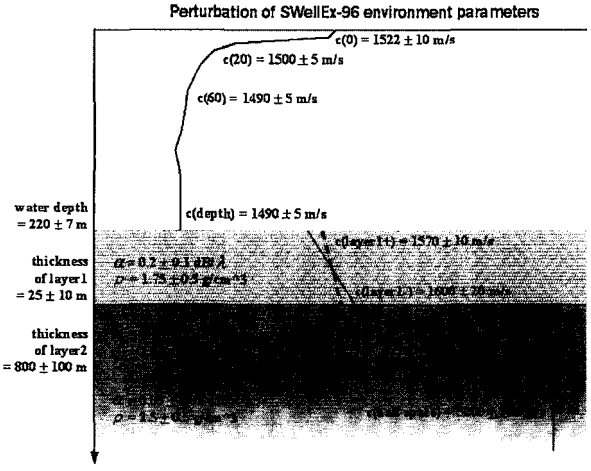

Fig. 6. Perturbed environmental parameters for the SWellEx-96 experiment.

show similar detection performance as the results using three layer bottom model. However, it is easier to construct the random replica set than three layer bottom model. We referenced geoacoustic parameters of half space bottom model that are derived for 49 Hz in [11] as the basis parameters (wave speed = 1598 m/s, density = 1.83 g/cm^3). And perturbed parameters were used to construct the random replica sets (wave speed = 1600 + 20 m/s, density = 2.0 + 0.5 g/cm^3, attenuation = 0.18 + 0.05 dB/km Hz, water depth = 218 + 5 m).

4.2. 2nd Set of Tones

Due to relatively low SNR of 2nd set of tones, some of narrow band processing results did not show good detection performance. Especially in the low frequency band, the components of strong interference from surface ship obstructed the source detection. Figure 7 shows the processing results incoherently integrated over ambiguity surfaces of some frequency tones. From these results, we can see that WNC used the best available environmental parameters while FEM used perturbed parameters to construct replicas (M=30). The ambiguity surface of FEM has the peak point at true source position in spite of relatively high level background noise field. However, WNC result shows the peak point at 3.4 km range located at the surface, which is the position of interference ship. Dynamic range was lowered to 5 dB for comparison.

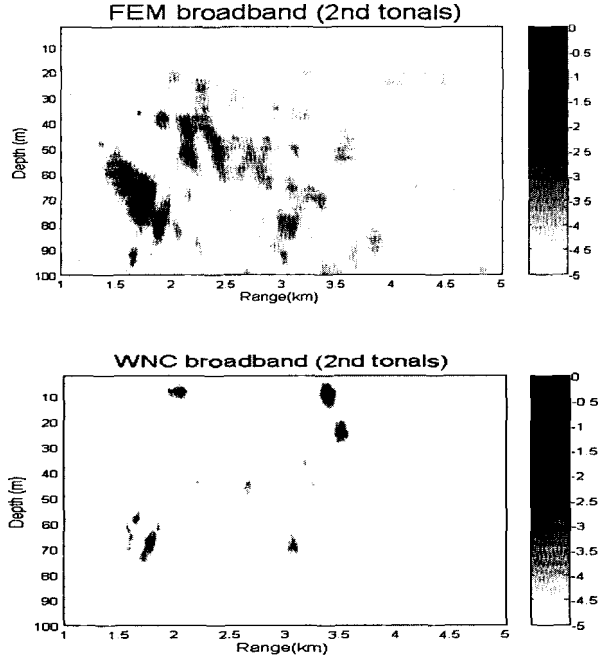

Fig. 7. Ambiguity surfaces of FEM and WNC for the 2nd set of tones. FEM and WNC results were integrated over 3 frequencies (151, 169 and 204 Hz). Dynamic range is 5 dB.

It is known that the eigenvectors of the CSDM measured on a vertical line array corresponds to the mode shapes [11]. In relation to received signal vector P of FEM, we used the integrated eigenvectors of CSDM (Eq. 10). Looking into the FEM processor, Eq. 8, the denominator is a product of received signal P and eigenvector matrix, E_s, from that dominant eigenvector is eliminated. But, in case of 2nd level signals which have low signal to noise ratio, the eigenvalues of CSDM spread out and so, signal P has relatively large noise components as well as source signal components. This produces loud background noise field in the ambiguity surface of FEM. Therefore, by constructing signal P by summing the eigenvectors from first to k-th (the number of dominant mode), we could obtain slightly better results. Figure 8 shows the square root eigenvalues of CSDM for frequency 130 (1st set of tones) and 133 (2nd set of tones) Hz. It can be seen that the eigenvalues of 133 Hz are more spread out than that of 130 Hz.

V. Summary and Conclusion

In this paper, we present FEM and WNC matched field processing results for real ocean experimental data. For high level signals, with deterministic environmental parameters, FEM processor was found to have similar AMS structure with that of Bartlett, but showed lower peak to noise-field ratio than Bartlett. In environmental mismatch case, MVDR_wnc processor had good sidelobe suppression ability

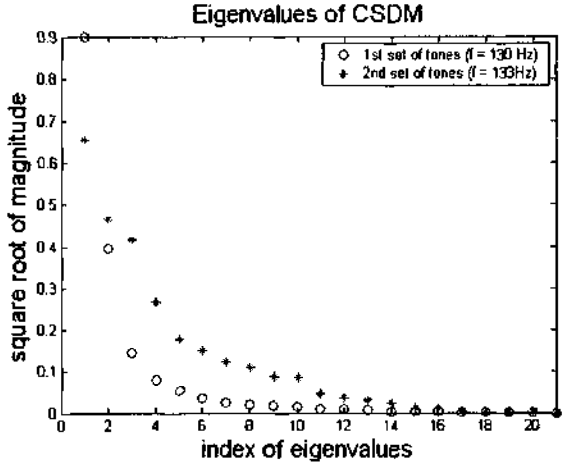

Fig. 8. A comparison of the eigenvalues of CSDM for 1st and 2nd set of tones (frequency 130 Hz and 133 Hz).

but, sometimes performed wrong localization. On the other hand, FEM processor showed robust source localization performance but, showed decreased peak to noise-field ratio. For relatively low level signals, although MVDR_wnc processor use deterministic parameters, it does not localize the true source position. FEM processor performed correct source localization with perturbed parameters but, peak to noise-field ratio was low.

In a word, FEM processor shows robust source localization performance in environmental mismatch case. And FEM has possibility of source localization for weak signal with perturbed environmental parameters. But, low peak to noise-field level in high frequency is a problem that still need to be resolved.

References

1. A. B. Baggeroer, W. A. Kuperman, and P. N. Mikhalevsky, "An overview of matched field methods in ocean acoustics," IEEE J. Oceanic Eng. 18, 401-423, Oct. 1993.
2. A. Tolstoy, *Matched Field Processing for Underwater Acoustics*, (World Scientific, Singapore, 1993).
3. H. Schmidt, A. B. Baggeroer, W. A. Kuperman, and E. K. Scheer, "Environmentally tolerant beamforming for high-resolution matched field processing: Deterministic mismatch," J. Acoust. Soc. Amer. 88 (4), 1851-1862, 1990.
4. J. A. Shorey, L. W. Nolte, and J. L. Krolik, "Computationally efficient Monte Carlo estimation algorithms for matched field processing in uncertain ocean environments," J. Comput. Acoust. 2 (3), 285-314, 1994.
5. A. M. Richardson and L. W. Nolte, "A posteriori probability source localization in an uncertain sound speed, deep ocean environment," J. Acoust. Soc. Amer. 89 (5), 2280-2284, 1991.
6. W. Seong and S. Byun, "Robust matched field processing algorithm based on feature extraction," IEEE J. Oceanic Eng. 27 (3), 642-652, July 2002.
7. H. Cox, R. M. Zeskind, and M. M. Owen, "Robust adaptive beamforming," IEEE Trans. Acoust., Speech, Signal Process. ASSP-35 (10), 1365-1376, Oct. 1987.
8. R. A. Gramann, *ABF algorithm implemented at ARL:UT*, Applied Research Laboratory, (Univ. of Texas, May 1992).
9. E. K. Westwood, *ORCA version 1.0 user's guide*, Applied Research Laboratory, (Univ. of Texas, 1998).
10. SR-113, H. Schmidt, *SAFARI: Seismo-Acoustic Fast field Algorithm for Range-Independent environments. User's Guide*, (SACLANT Undersea Research Center, La Spezia, Italy, 1987).
11. P. Hursky, W. S. Hodgkiss, and W. A. Kuperman, "Matched field processing with data-derived modes," J. Acoust. Soc. Amer. 109 (4), 1355-1366, 2001.

[Profile]

•Kyungseop Kim

2002, Dept. of Naval Architecture and Ocean Eng., Seoul Nat'l Univ. (B.S.)

2002~Present, Doctoral Course in Dept. of Naval Architecture and Ocean Eng., Seoul Nat'l Univ.

※Areas of interest: Matched field processing, Geo-acoustic inversion

•Woojae Seong

1982, Dept. of Naval Architecture, Seoul Nat'l Univ. (B.S.)

1990, Dept. of Ocean Engineering, M.I.T. (Ph. D.)

1991, MIT Post-doctoral Associate

1992, Professor, Dept. of Ships and Ocean Eng., Inha Univ.

1996, Professor, Dept. of Ocean Eng., Seoul Nat'l Univ.

※Areas of interest: Propagation modeling, Geo-acoustic inversion, Matched field processing, Acoustic monitoring, Sonar applications for AUV

•Heechun Song

1978, Dept. of Naval Architecture, Seoul Nat'l Univ. (B.S.)

1980, Dept. of Naval Architecture, Seoul Nat'l Univ. (M.S.)

1990, Dept. of Ocean Engineering, M.I.T. (Ph. D.)

1991-1995, Korea Ocean Research and Development Institute

-Present, Marine Physical Lab./Scripps Institution of Oceanography, UCSD

※ Areas of interest: Time-reversal acoustics, Robust matched field processing, Wave propagation physics